Chapter 4: Binary Mixtures - Evaluation of the Experimental Results

Homogenous freezing of water + non-electrolyte mixtures at low temperatures have been studied by several authors until now (Angell 1983; Oguni and Angell 1983; Koop, Luo et al. 2000; Koop 2004; Miyata and Kanno 2005). In this manner, the homogenous nucleation temperatures (T_H) have been characterized for various non-electrolytes; and their affects on the nucleation behaviour of liquid water have been investigated. Oguni and Angell (Oguni and Angell 1983)studied the hydrophilic and hydrophobic solute effects on T_H. They concluded that the solutes have additive contributions from each functional group they have. In contrast Koop et al (2000) (Koop, Luo et al. 2000) proposed that the homogeneous nucleation of ice from a supercooled aqueous solution is independent of the nature of a solute but depends only on the water activity of the solution. This proposal is more recently challenged by Miyata and Kanno's (Miyata and Kanno 2005) measurements on the homogeneous nucleation temperatures of aqueous solutions of alcohols and sugars. Similar to Oguni and Angell's conclusions, Miyata and Kano concluded that there is a linear relation between T_H and the number of OH groups in an alcohol molecule.

In this work, the homogeneous nucleation behaviours of supercooled aqueous non-electrolyte solutions are investigated by the levitated single droplet experiments, and their nucleation rates are measured. A detailed list is given in Table 4.1, which shows the non-electrolytes that are used in the experiments. The concentration ranges of solutes are also given.

Table 4.1: The list of solute substances used in carrying out the nucleation rate experiments in aqueous solutions. The experiments are carried out at different solute concentrations for each substance. The concentrations are expressed in mole fractions in the second column.

Non-electrolyte solute	Mol fraction of the solute (x_2)
Ethanol	0.002, 0.01[(a)]
Isopropanol	0.002
Glycol	0.002, 0.003, 0.023, 0.047
1,4 - Dioxane	0.002, 0.041, 0.133, 0.163, 0.207, 0.3, 0.363, 0.475
Urea	0.002, 0.01, 0.02

[(a)] Measured by Kabath (Kabath 2006).

The solute concentrations are stated as mol fractions (x_2), since it is convenient to compare the compositions of different binary liquid mixtures, in terms of the ratio of number of solute molecules to the number of water molecules. By this way, the relative contribution of molecular weights and temperature-dependent molar volumes in the comparisons are disregarded.

4.1 Anomalies Observed in the $\ln(N_u/N_0)$ vs. $V_d \cdot t$ Diagrams

The ln (N_u/N_0) vs. $V_d \cdot t$ diagrams show substantial deviations from the expected linear behaviour in some cases. This was previously noted by Stöckel (Stöckel 2001) for supercooled liquid water and heavy water. However, such distinguishing features are observed more frequently and in a diverse way for binary aqueous mixtures of non-electrolytes. These features have also complicated the analysis of nucleation rates from the nucleation-time statistics. For this reason, it deserves particular attention to reveal these puzzling features.

In the interpretation of nucleation rates from the droplet freezing statistics equation (4-1) is used to describe the decay of supercooled liquid phase into solid phase:

$$\ln(N_u/N_0) = - J(T) \cdot V_d \cdot t \qquad (4\text{-}1)$$

N_u : Number of unfrozen droplets at the time "t" after injection of the droplet.
N_0 : Total number of supercooled water droplets.
V_d : Volume of the droplet.
J(T): Rate of ice nucleation at temperature T.

According to above equation, the decay of unfrozen droplets is linear with respect to $V_d \cdot t$, and the slope of the ln (N_u/N_0) vs. $V_d \cdot t$ plot gives the temperature dependent nucleation rate J(T) for the ideal case. The deviations from the linear behaviour that occur in ln (N_u/N_0) vs. $V_d \cdot t$ diagrams are classified in the following way, according to the features they represent:

i. Minor deviation from the linearity that appear at the long time region.

ii. Minor deviations from the linearity in some parts of an ln (N_u/N_0) vs. $V_d \cdot t$ diagram.

iii. ln (N_u/N_0) vs. $V_d \cdot t$ diagrams having two linearly progressing regions, which results in occurrence of a "knick".

iv. A plateau or a broader flat region occurring for the very beginning of an ln (N_u/N_0) vs. $V_d \cdot t$ diagram.

v. ln (N_u/N_0) vs. $V_d \cdot t$ diagram being not linear but having a curved shape where the long-time region decreases rapidly.

The first two features listed above are recognized as experimental artefacts. The minor deviations that are observed at the long time region (**i**) usually occur as a result of $V_d \cdot t$ product being measured lower than the expected value. This is mostly because a very long lasting droplet looses its stability and escapes the trap. However, the evaluation electronics can not distinguish this situation. Consequently the moment of the escape is interpreted as the moment of nucleation. This results in incorrect values for the registered nucleation times for long-living droplets.

The partial deviations from the linear behavior in (**ii**) can be weighed down simply by collecting sufficiently high number of droplets for statistical analysis.

The occurrence of "knick" s in (**iii**) is first mentioned by Stöckel (Stöckel 2001) for liquid water and heavy water. They are reported to occur at the warmer ends in a temperature interval, for which the nucleation behaviours of supercooled liquid H2O and D_2O are investigated. In such cases the ln(N_u/N_0) vs. $V_d \cdot t$ diagrams have two linear segments (see also Figure 4.1). The segment having the higher slope is observed for the short time region, which corresponds to the lower values of $V_d \cdot t$ products on the x-axis. This segment contains in most cases 95 % of the experimental points. A second linear segment develops at rather long nucleation times with a lower slope, which is evaluated as long-time region. The statistical weights of the long-time regions are fairly low in comparison to the short-time regions; they rarely exceed 5 % of the total number of experimental points.

New measurements especially that are performed with water + 1 4-dioxane liquid mixtures show diversity in the qualification of short and long time regions. For instance, the long-time regions appear with higher statistical weights, even beating the short-time region, in some cases. Additionally the long-time regions in some cases may have higher slopes than that of the short-time regions. Therefore, the feature described in (**iii**) is appeared to be more characteristic which seems to be originating from the nature of nucleation event for binary systems.

The plateau formation that is described by the feature (**iv**) is observed almost in all cases of the current measurements. They are also reported earlier by Stöckel especially for the measurements, which are carried out at the cooler ends of the temperature intervals.

Two parameters characterize the plateau formations in the $\ln(N_u/N_0)$ vs. $V_d \cdot t$ diagrams. The first parameter is the minimum of $V_d \cdot t$ values, which determines the beginning of the plateau region. The second parameter is the deviation of the intercept of the best fit-line from the zero value on the y-axis, which is correlated with the extent of the plateau region. The use of minimum $V_d \cdot t$ value and the intercept in defining the plateau formation, is demonstrated in Figure 4.2.

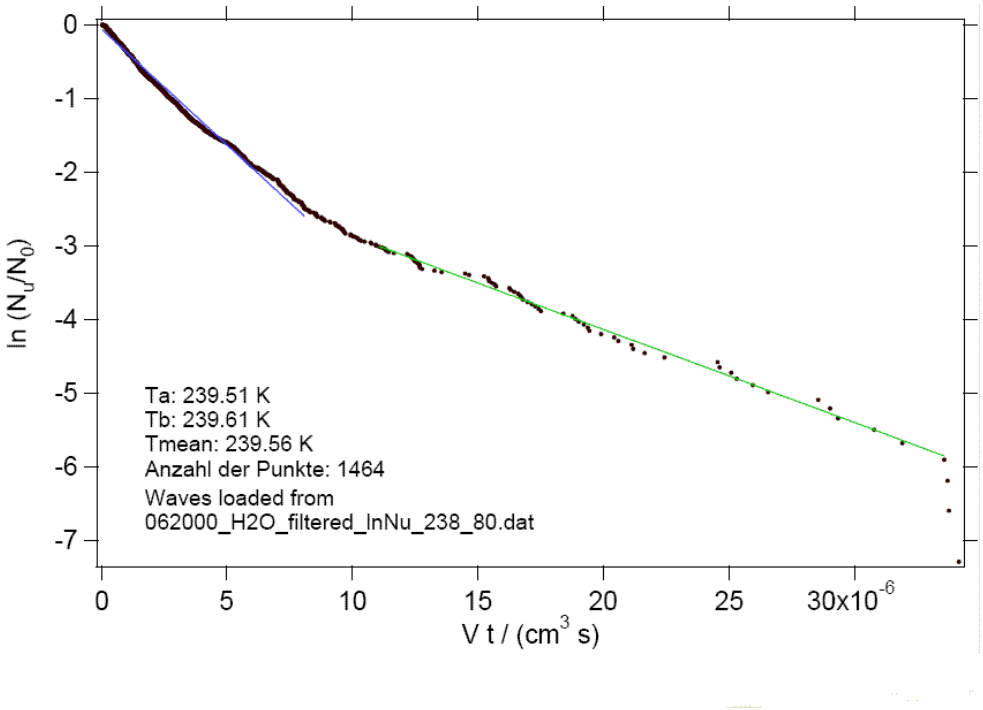

Figure 4.1: A knick that appears in the ln (N_u/N_0) vs. $V_d \cdot t$ diagram for the nucleation rate measurement of supercooled liquid water at a constant temperature. The short-time region, which is made clear by a blue line, has a higher slope, i.e. higher nucleation rate. The long-time region is signified by a green line. It has a lower slope, so that it implies a lower nucleation rate. A sum of 1464 droplets is analyzed to obtain above diagram. The number of droplets that belong to the long-time region is not more than a hundred, having a much less statistical weight in comparison to the short-time region. Besides, the last three data points in the diagram can be given as an example to the experimental artifact described in (i).
After (Stöckel 2001).

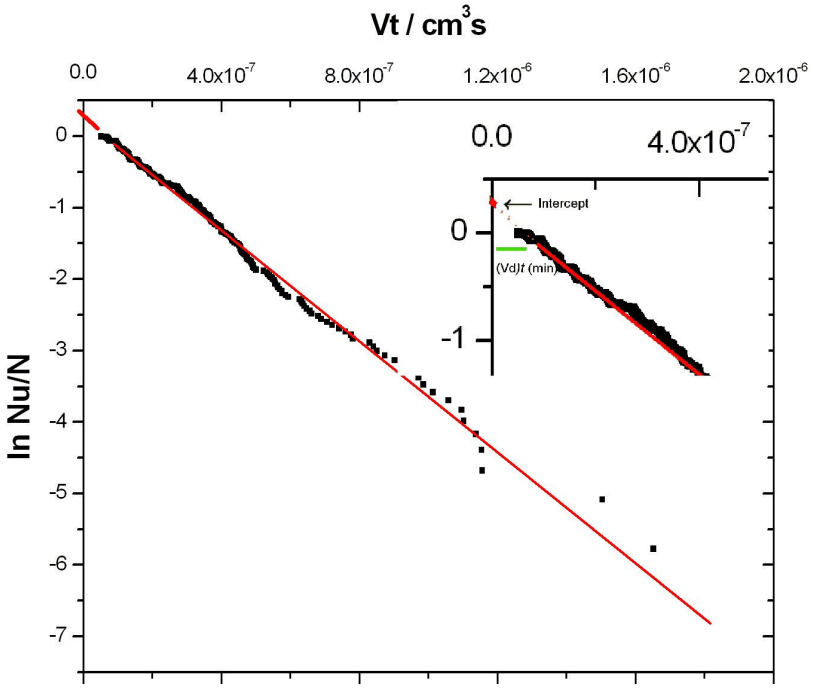

Figure 4.2: The ln (N_u/N_0) vs. V_d·t diagram obtained from the measurement of the nucleation times in supercooled liquid water at -36.16 °C. Note the occurrence of a small flat region. The use of minimum value of V_d·t and the deviation of the intercept from the origin, in defining the plateau formation is shown in detail in the inset.

One point of view for the explanation of this feature is the presence of an induction time. It is based on the assumption that a droplet requires some time to come into thermal equilibrium with the surrounding atmosphere, in a temperature jump experiment. In this respect, the minimum of V_d·t values obtained from current measurements of ice nucleating rates in supercooled liquid water are found to be consistent with the previously calculated values of induction times (0.5s). (Stöckel, Weidinger et al. 2004) In water + non-electrolyte mixtures this value may differ depending on the nature of solution, since the calculation of induction times requires the knowledge of the viscosity of a solution.

Feature (**v**) is characterized by the development of a broader flat region which is particularly observed for water + 1,4-dioxane liquid mixtures at a dioxane mol fraction of $x_2 = 0.04$ (see also Figure 4.3). This kind of nucleation behaviour is previously obtained for long-chain n-alkane micro droplets. There, this feature was interpreted as a sign of "surface nucleation" and the ln (N_u/N_0) vs. V_d·t diagrams were fitted to an Avrami-type equation that includes a time-dependent surface-term (Weidinger, Klein et al. 2003; Weidinger 2003).

More than one of the above listed anomalies can be present in some of the diagrams. The nature of the solution under test may lead to complicated statistics, which make it difficult to analyze the nucleation rates methodically. To be able to further discuss on the reasons that lie behind the anomalies that are produced in the new measurements, the relation between the nature of a particular anomaly and the nature of the solution should be well identified.

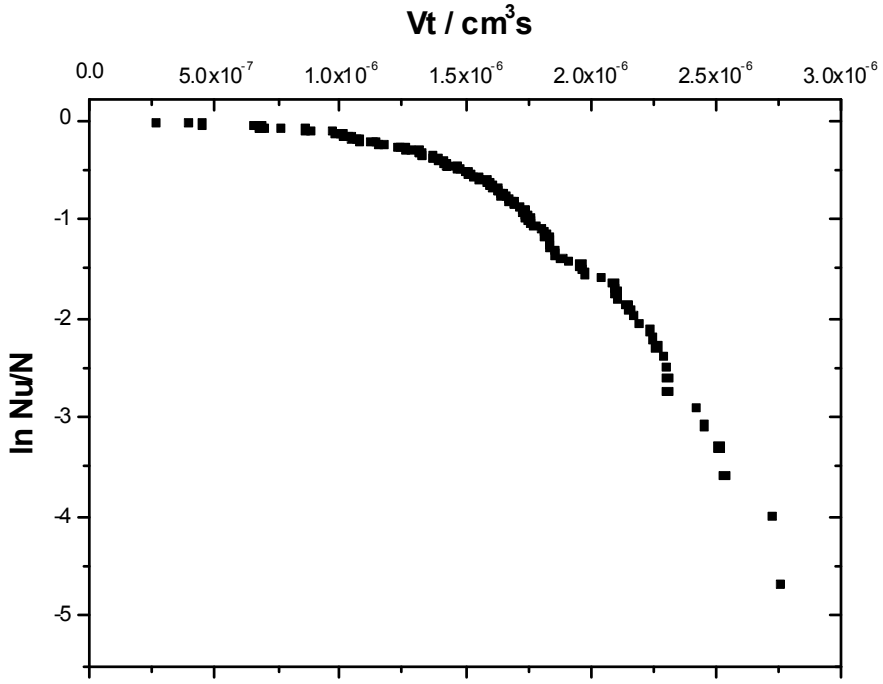

Figure 4.3: An exemplary case to feature (v), which is characterized by the formation of a broad flat region for the short-time statistics. The diagram is obtained from the ice nucleation time measurements of water + 1,4-dioxane liquid mixture (x_2 = 0.04) at -43.29 °C. Similar diagrams were reported for long-chain n-alkane microdroplets previously.

4.2 Measurements of Homogenous Nucleation Rates

4.2.1 Measurements at Low Solute Concentrations:

The low-solute-concentration parts of the homogenous ice nucleation measurements are performed with the mole fraction of the solutes $x_2 = 0.002$. At a mole fraction of 0.002, there is 1 solute molecule per 500 water molecules in a liquid mixture. This implies that the ice nucleation of the water molecules govern the dynamics of phase change. Besides, the association of solute molecules can be ignored at such a low solute concentration.

The effect of ethanol (C_2H_5OH), isopropanol (C_3H_7OH), glycol $C_2H_4(OH)_2$, 1,4-dioxane ($C_4H_8O_2$) and urea $(NH_2)_2CO$ on the nucleation behaviour of liquid water is investigated in relation to the number and property of H-bonding groups they contain. The temperature dependence of nucleation rates are plotted in Figure 4.4. For comparison reasons, the temperature dependence of pure liquid water is also given, which is obtained from the recent measurements of nucleation times in two different traps. The results of the measurements for liquid mixtures are also summarized in Table 4.2 with further experimental details.

The ratios of J_{H2O}/J_{mix} of the different low concentration mixtures show no significant temperature dependence. The differences of the values given in the last column of Table 4.2 are in the error limit of the evaluation of J. However, averaging the values reveal different results for different solutes. The averaged values for water/dioxane and water/glycol are 5.80 and 6.24 respectively. The values for ethanol, isopropanol and urea are 1.65, 1.83 and 1.73. These values imply that ethanol, isopropanol and urea reduce the nucleation rate nearly at the same degree at a mole fraction of $x_2 = 0.002$. On the other hand a more significant reduction occurs in the case of 1, 4-dioxane and glycol.

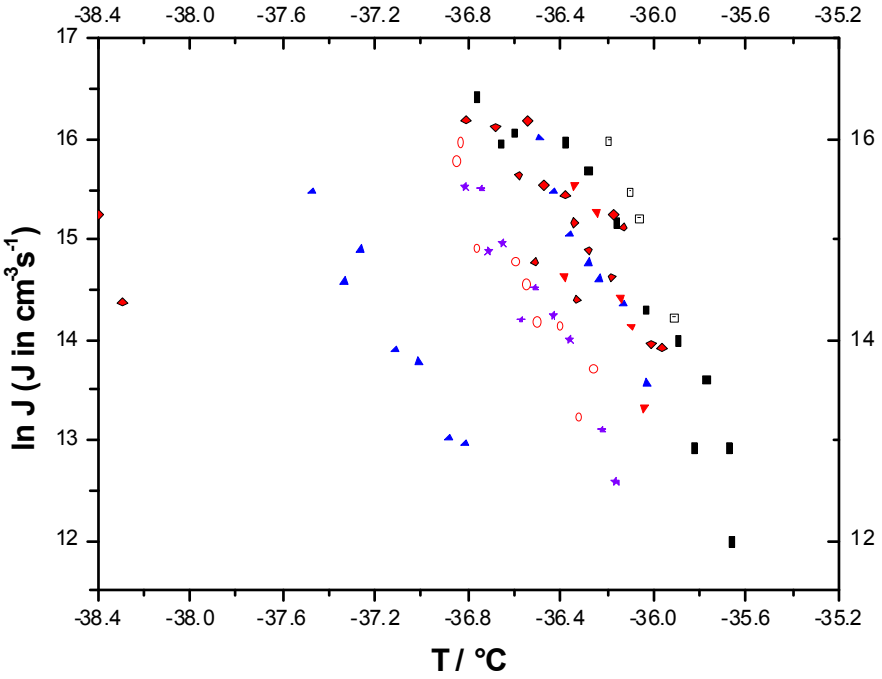

Figure 4.4: Temperature dependence of nucleation rates for supercooled water + non-electrolyte systems at low solute concentrations. (black squares: pure water -trap A, empty squares: pure water - trap B, blue triangles: water + ethanol at $x_2 = 0.002$ & $x_2 = 0.01$, red-inverted triangles: water + isopropanol, purple stars: glycol, red circles: water + dioxane, black-red diamonds: water + urea at $x_2 = 0.002$ & $x_2 = 0.01$) The ethanol measurements at $x_2 = 0.01$ were conducted by Petr Kabath.

It is somewhat unexpected that 1 solute molecule per 500 water molecules effects the nucleation rates of ice. From these experimental results we conclude that the solute molecules are enriched in the interface in between the patches. Therefore, they become more effective, and slow down the process of ice nucleation by sticking on the growing sites of the agglomerates on the surface of the patches. A higher reduction of J in water/dioxane and water/glycol mixtures is attributed to the higher number of H-bonding sites contained by these molecules.

A special comment is required for the system urea/water. When planning the experiments, we expected urea to have a very strong influence on J, because it has been reported in the literature that it has structure breaker properties (Franks 1973). We observed at low concentrations that urea has a similar effect with ethanol and isopropanol. We explain these results by two arguments:

Table 4.2 Homogeneous nucleation rates of ice in aqueous solutions of non-electrolytes at low solute concentrations. The standard deviation of the fit for water values is 0.26816 for ln J = aT + b.

Liquid mixture: water/dioxane, at x_2 = 0.002

T_{meas}	J_L	Intercept	J_R	# drops	J_{H2O}	J_{H2O}/J_{mix}
-36.26	9.12E+05	0.043	-	239	4.17E+06	4.57
-36.32	5.66E+05	0.013	-	207	5.16E+06	9.11
-36.4	1.39E+06	0.088	-	249	6.84E+06	4.92
-36.5	1.45E+06	0.184	-	228	9.74E+06	6.72
-36.55	2.11E+06	0.235	-	215	1.16E+07	5.51
-36.59	2.65E+06	0.155	-	183	1.34E+07	5.05
-36.76	3.03E+06	0.196	-	223	2.44E+07	8.06
-36.83	8.70E+06	0.531	-	188	3.13E+07	3.60
-36.85	7.18E+06	0.565	-	317	3.36E+07	4.68

Liquid mixture: water/ethanol, at x_2 = 0.002

T_{meas}	J_L	Intercept	J_R	# drops	J_{H2O}	J_{H2O}/J_{mix}
-36.03	7.82E+05	0.048	-	110	1.85E+06	2.36
-36.13	1.71E+06	0.017	-	170	2.63E+06	1.54
-36.23	2.21E+06	0.191	-	208	3.75E+06	1.70
-36.28	2.60E+06	0.206	-	187	4.48E+06	1.72
-36.36	3.44E+06	0.313	-	158	5.94E+06	1.73
-36.43	5.24E+06	0.342	-	234	7.61E+06	1.45
-36.49	8.93E+06	0.495	-	156	9.41E+06	1.05

Liquid mixture: water/isopropanol, at x_2 = 0.002

T_{meas}	J_L	Intercept	J_R	# drops	J_{H2O}	J_{H2O}/J_{mix}
-36.04	6.12E+05	0.031	-	169	1.92E+06	3.13
-36.09	1.38E+06	0.064	-	202	2.29E+06	1.66
-36.14	1.82E+06	0.193	-	248	2.73E+06	1.50
-36.24	4.30E+06	0.165	-	148	3.89E+06	0.90
-36.34	5.57E+06	0.062	-	86	5.53E+06	0.99
-36.38	2.25E+06	0.064	-	215	6.37E+06	2.83

Table 4.2 – Continues

Liquid mixture: water/glycol, at $x_2 = 0.002$

T_{meas}	J_L	Intercept	J_R	# drops	J_{H2O}	J_{H2O}/J_{mix}
-36.16	2.95E+05	0.043	-	159	2.93E+06	9.93
-36.22	4.92E+05	0	-	148	3.62E+06	7.36
-36.36	1.21E+06	0.084	-	205	5.94E+06	4.91
-36.43	1.54E+06	0.063	-	157	7.61E+06	4.94
-36.51	2.02E+06	0.115	-	192	1.01E+07	5.00
-36.57	1.47E+06	0.082	-	187	1.25E+07	8.49
-36.65	3.12E+06	0.289	-	183	1.66E+07	5.31
-36.71	2.88E+06	0.13	-	516	2.05E+07	7.11
-36.74	5.45E+06	0.32	-	265	2.28E+07	4.18
-36.81	5.54E+06	0.422	-	297	2.92E+07	5.26

Aqueous Solution: water/urea, at $x_2 = 0.002$

T_{meas}	J_L	Intercept	J_R	# drops	J_{H2O}	J_{H2O}/J_{mix}
-35.96	1.11E+06	0.093		177	1.44E+06	1.30
-36.01	1.15E+06	0.097		146	1.72E+06	1.50
-36.13	3.71E+06	0.1		154	2.63E+06	0.71
-36.17		0.403	4.20E+06	135	3.03E+06	0.72
-36.18		0.2	2.25E+06	117	3.14E+06	1.40
-36.28	2.93E+06	0.351		219	4.48E+06	1.53
-36.33	1.79E+06	0.057		115	5.34E+06	2.98
-36.34		0.324	3.88E+06	199	5.53E+06	1.43
-36.38		0.417	5.09E+06	149	6.37E+06	1.25
-36.47	5.61E+06	0.286		165	8.76E+06	1.56
-36.51	2.62E+06	0.093		228	1.01E+07	3.85
-36.54		1.159	1.07E+07	130	1.12E+07	1.05
-36.58	6.19E+06	0.215		163	1.29E+07	2.09
-36.68	1.00E+07	0.581		273	1.84E+07	1.84
-36.81	1.08E+07	0.557		178	2.92E+07	2.70

1. Like the other solutes, urea is mainly dissolved /enriched in the interface, which contains mostly the non-bonded water molecules.
2. The amino groups of urea molecule can not simultaneously bind to the surface of agglomerates, which are found on the surface of the patches.

Indeed, we find a support to our conclusion in the second statement from another independent experimental study (Rezus and Bakker 2006). In this study it is shown that only one of the water molecules in the solvation shell of a urea molecule binds strongly to the urea molecule.

The nucleation statistics were usually good at low solute concentrations. However, for the warmer ends of the temperature intervals, the statistics were disturbed at the long time regions in the ln (N_u/N_0) vs. $V_d \cdot t$ diagrams. This was due to difficulties in levitating droplets for long durations. The droplets lost their stability if they survived freezing for more than 80 seconds. During this time, the volume of a droplet was reduced rapidly by a series of Coulomb explosions. Eventually jet formation and the escape of the droplet from the trap were observed. Since it happened particularly for liquid mixtures, it seems to be remarkable. It was not experienced earlier with pure liquid water.

The reduction of the volume of an unfrozen droplet is shown in Figure 4.5 for water + isopropanol liquid mixture at a solute concentration of $x_2 = 0.002$. As seen from the figure the droplet losses about 40 percent of its initial volume at the end of 80 seconds. Such a volume reduction can not be compensated by the evaporation of single molecules on the surface of droplet, at these conditions. Therefore this result supports the explanation of the loss of stability of long-living droplets with the occurrence of Coulomb explosions.

At the warmer ends of the temperature intervals, the nucleation rates are on the order of 10^5 germs per cubic centimetre per second. This means many droplets would normally survive freezing, longer than 80 seconds. Therefore, it is unavoidable that the long time regions in the ln (N_u/N_0) vs. $V_d \cdot t$ diagrams are disturbed. In those cases the nucleation rate is taken to be the slope of short-time regions.

Somewhat poorer statistics for the aqueous urea solutions at this concentration can be ascribed to the precipitation of urea crystal on the tip of the injectors. The precipitation of urea can lead to fluctuations in the actual urea concentrations and affect the nucleation times. These events disturb the experiments and lead to poorer droplet nucleation statistics.

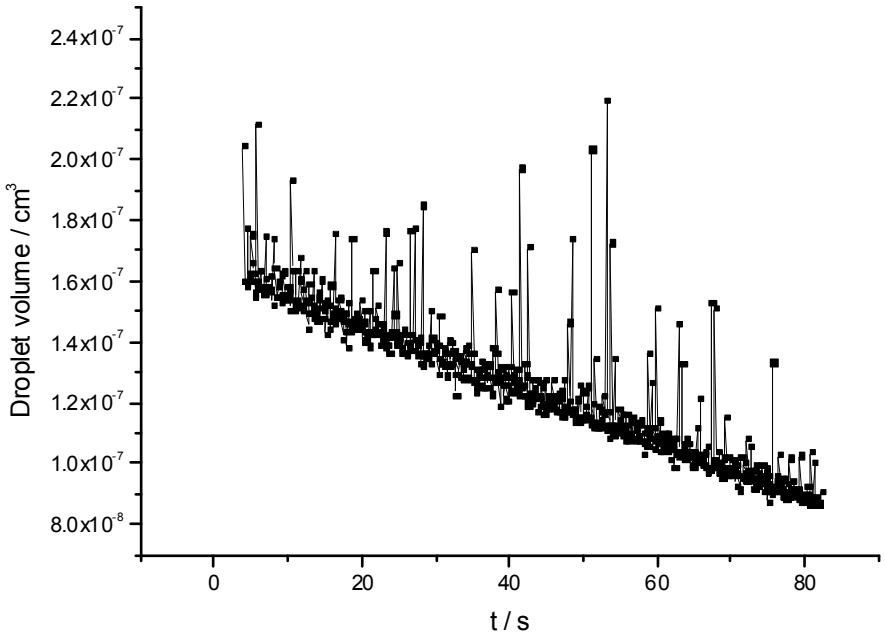

Figure 4.5: The reduction of volume of an unfrozen droplet obtained from the experiment performed at -36.04 °C in supercooled liquid mixture of water + isopropanol at x_2 = 0.002. The volume reduction reaches up to 40 % of the initial volume in 80 seconds.

4.2.2 Measurements at Higher Solute Concentrations

4.2.2.1 Water + Glycol

Above x_2 = 0.01 the nucleation rates for the water + glycol system can not be determined, since the droplets freeze very rapidly or they do not freeze over long-times. Especially at colder temperatures the droplets could be steadily levitated more than 500 seconds, which puts contrast to the frequent stability loses mentioned for the measurements conducted at low solute (x_2 =0.002) concentrations. Exemplary cases to the freezing anomalies obtained for the nucleation time measurements of water + glycol mixtures, are given in Figures 4.6 and 4.7.

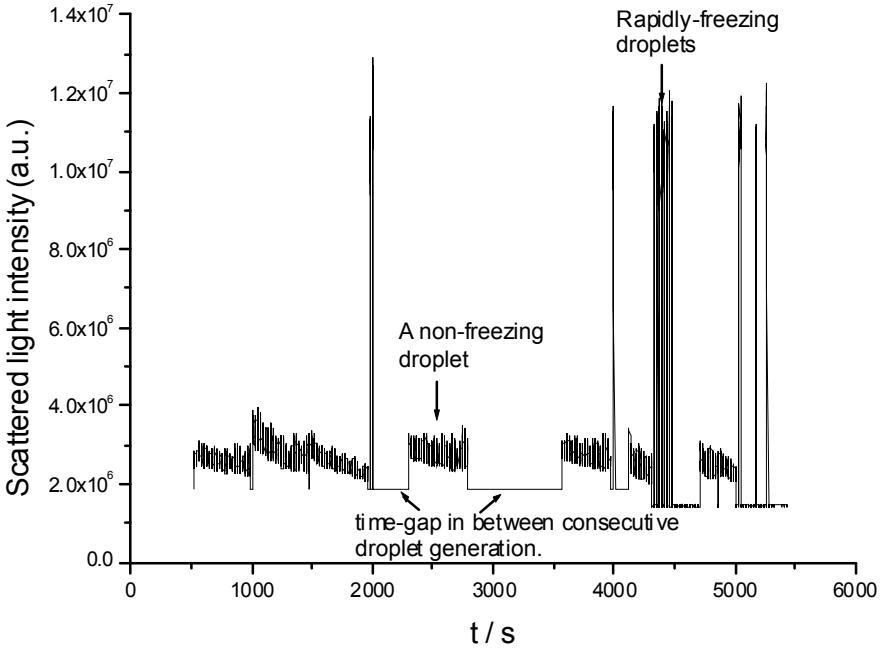

Figure 4.6: The scattering light intensity obtained from the first 35 droplets in water +glycol system at x_2 = 0.047 at T = -56.24 °C.

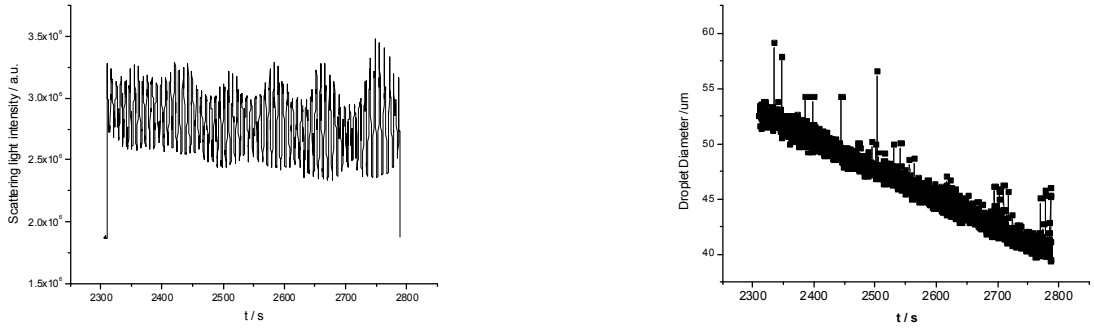

Figure 4.7: A droplet which is not freezing in 500 s and the change of droplet's diameter in time.

Although the nucleation rates can not be determined for higher glycol concentrations in liquid water, the temperature intervals, in which the sudden freezing events occur, can be taken as the limit of homogenous nucleation temperatures T_H. These temperature intervals are given in Table 4.3:

Table 4.3: Homogenous nucleation temperatures (T_H) in water + glycol liquid mixtures at $x_2 = 0.01$, $x_2 = 0.02$ and $x_2 = 0.05$.

Concentration of glycol in mol percents	Temperature interval/ °C
0.01	around (-39)
0.023	(-43.8) – (-46)
0.047	(-54) – (-58)

The droplets which are not freezing in long durations point to the gel like glassy material in the droplet. The fact that these observations had been made only in some of the droplets implies a statistical nature of the occurrence of these events.

If we refer back to the diagram in Figure 1.7 for the phase relations of liquid water, we see that the temperature interval of the freezing anomalies observed with water + glycol liquid mixtures at $x_2 = 0.02$ fall near to the debated singularity temperature T_s of metastable liquid water. On the other hand the temperature interval of measurements performed with liquid mixtures of water + glycol at x_2 0= 0.05 falls in the LDL domain of liquid water, which can not be accessed with pure water samples.

From these information, it is suggested that large density fluctuations occur in the droplets of water + glycol mixtures. For droplets of such small size these fluctuations could dominate the nature of events occurring in the droplets. Therefore these droplets may alter glass transition.

4.2.2.2 Water + 1, 4-dioxane

From the non-electrolyte solutes used in this study 1, 4-dioxane was proven to be a good candidate to conduct the nucleation rate experiments over a wide range of concentration in liquid mixtures of water. 1,4-dioxane is a cycloether, macroscopically miscible with water at any ratio. It is liquid at room temperature, which makes it easy to handle as a solute at higher concentrations in comparison to a solid substance such as urea. Dioxane is also not as volatile as ethanol and isopropanol; therefore we do not need to worry about the alteration of liquid-mixture composition during the measurements.

Although no hydrogen bond can be formed among dioxane molecules, a dioxane molecule conducts good hydrogen-bond acceptor functionality through its oxygen atoms when mixed with water molecules. Structural investigation of water + dioxane mixtures by various thermodynamic methods(Malcom and Rowlinson 1957; Schott 1960; Sakurai 1992), as well as infrared and Raman spectroscopy(Errera, Gaspart et al. 1940; Tominaga and Takeuchi 1996), dielectric relaxation(Clemett, Forest et al. 1964; Gark and Smyith 1965; Atkinson, Rajagopaian et al. 1981; Mashimo, Niura et al. 1992), NMR(Fratiello and Douglass 1963; Hindman, Svirmickas et al. 1968; Goldammer and Hertz 1970; Takamuku, Nakamizo et al. 1998), dynamic light scattering(Sorensen 1988; Yang, Li et al. 2004) and computer simulations(Cadioli, Gallinella et al. 1993; Sitraibl, Baumruk et al. 1998) point out to three important type of water/dioxane interactions:

I. At low mol fractions of dioxane ($x < 0.1$) some of the dioxane molecules are embedded inside the water network that disturbs the structure.
II. At high concentrations ($x > 0.2$) dioxane breaks the H-bonding of water network, and the pentamer structure of water disappears.
III. With even higher concentration ($x > 0.3$) the disruption will lead to monomeric form of water molecules, which interact with the oxygen atoms of dioxane.

A recent study on solvation dynamics of Coumarin 153 dye in dioxane + water solvent system by fluorescene spectroscopy(Molotsky and Huppert 2003) identify oligomers composed of

dioxane – water molecules as a result of strong association. On the other hand there are other studies of light scattering from water + dioxane mixtures which show that the mixture is not microscopically homogeneous(Yang, Li et al. 2004).

The nucleation rate measurements in water + dioxane system were performed for the following mol fractions of dioxane in water:

x_{diox} = 0.04, 0.13, 0.14, 0.16, 0.21 0.30, 0.36 and 0.48

We also tried to perform measurements with higher mol fractions ($X_{diox} > 0.5$); however it was hardly achievable to trap a droplet, possibly because of not being able to establish high enough ionic charge on the droplet's surface with the current charging scheme.

In order to identify the compositions of water + dioxane mixtures, a liquid to solid phase diagram at ambient pressure is given in Figure 4.8. The diagram consists of the melting points of water + dioxane mixtures plotted against the mol percentage of dioxane in the mixture.

The melting point data is taken from earlier studies of Unkovskaya (Unkovskaya 1913) The dioxane concentrations at which the nucleation rate experiments were carried out are indicated by red squares . From the diagram it is seen that the mixture has an eutectic point at B (**x_2: 0.155, T: -15.4 ^oC**). At the temperature of eutectic point the chemical potentials of liquid water, ice, liquid dioxane and solid dioxane are the same. Therefore the liquid to solid phase transitions take place simultaneously for both water and dioxane.

Within the region A-D-B the liquid mixture will be supersaturated with respect to water. A new equilibrium will be established on the liquidus curve A-B followed by ice nucleation. On the other hand, the liquid mixture will be supersaturated with respect to liquid dioxane, in the region C-B-E. The equilibrium will be established after the nucleation of dioxane crystals, and the equilibrium point will be shifted to lower values of dioxane concentration on the liquidus curve C-B.

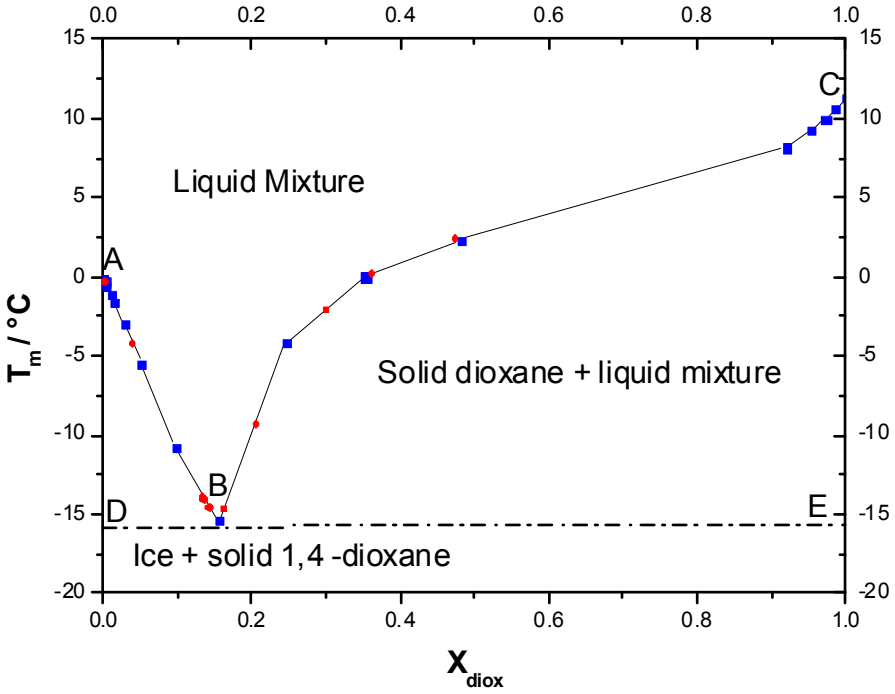

Figure 4.8: The equilibrium melting points for water + 1, 4-dioxne liquid mixture.

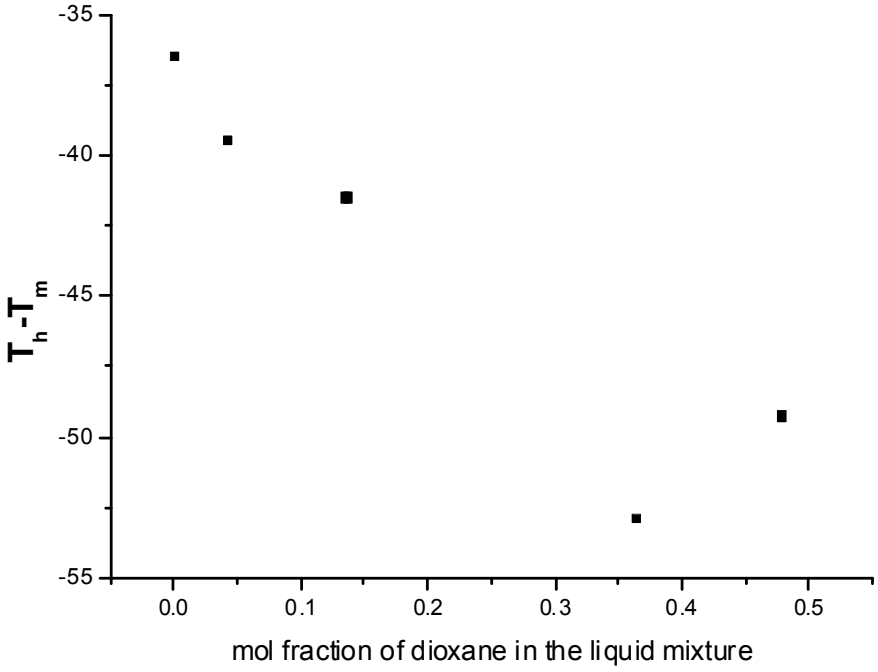

Figure 4.9: The degree of supercoolings required to obtain a nucleation rate of J = 3 E6 at various mole fractions of 1,4-dioxane for water/dioxane binary liquid mixtures.

Below -15.4 ^{o}C (the eutectic point temperature) the only thermodynamically stable phase will be the solid mixture of dioxane and ice. Therefore, cooling the liquid mixture below this point, we will have the metastable liquid phase, which is saturated both in liquid water and dioxane.

All the ln (N_u/N_0) vs. $V_d \cdot t$ diagrams obtained from the measurements of nucleation times in water + dioxane liquid mixtures are given in Appendix D. In addition, we present here the details of these measurements and the nucleation rates in Table 4.4.

In Figure 4.9 the supersaturations, i.e. the degree of supercoolings that we need to obtain a nucleation rate of J = 3 E6, in water/dioxane binary liquid mixtures are plotted. This figure demands that the nucleation rate J first reduces for increasing mole fraction of dioxane below x_2 = 0.30. After this mole fraction the nucleation rate enhances with increasing dioxane content.

With increasing solute concentration, it is expected that solute molecules enter the patches in liquid water, and create more lattice defects. The structure of liquid water may be completely broken after a certain solute concentration. According to Figure 4.9, this is expected to happen above x_2 = 0.30 for water/dioxane mixtures bringing a change in the nucleation mechanism. On the other hand, it is very difficult to quantify the effect of dioxane to ice nucleation in liquid water at high concentrations, according to the water model developed in Chapter 2. This is because; dioxane going into the patches may alter the transport properties of liquid water from one side, and may prevent the growth of agglomerates by sticking on their surface from the other side. Furthermore the freezing may not lead to the thermodynamically most stable system at high concentrations of dioxane.

Table 4.4: Homogenous nucleation rates in liquid mixtures of water + 1,4-dioxane at high dioxane concentrations.

Water + dioxane liquid mixture at x2 = 0.04

T_{meas}	$\|T_s\|$	J_L	Intercept	J_R	# drops
-43.30	39.10	5.95E+05	-0.139		85
-43.60	39.40	5.74E+05	-0.032	6.43E+05	120
-43.70	39.50	8.06E+06	-0.044	2.03E+06	185
-43.94	39.74	7.04E+06	0.289	3.80E+05	60
-45.17	40.97	6.02E+06	0.384		185

Water + dioxane liquid mixture at x2 = 0.133

T_{meas}	$\|T_s\|$	J_L	Intercept	J_R	# drops
-54.34	40.44	2.37E+05	-0.036	3.94E+05	121
-54.46	40.56	1.40E+06	0.109	2.51E+06	245
-54.55	40.65	1.67E+06	0.135	2.20E+06	81
-54.65	40.75		0.219	1.42E+06	168
-54.98	41.08		0.271	1.85E+06	127
-55.07	41.17	2.71E+06	0.334	7.42E+06	109
-55.10	41.20		-0.394	1.56E+06	61
-55.18	41.28	2.00E+06	0.102	4.40E+06	143
-55.28	41.38		0.420	4.73E+06	182
-55.51	41.61		0.150	4.49E+06	144
-55.64	41.74		0.179	3.25E+06	
-55.77	41.87	4.41E+06	0.120		243
-55.86	41.96	8.23E+06	0.162		198
-55.97	42.07	3.58E+06	0.217	5.13E+06	223
-56.16	42.26		0.718	2.32E+07	106

Water + dioxane liquid mixture at x2 = 0.136

T_{meas}	$\|T_s\|$	J_L	Intercept	J_R	# drops
-55.66	41.56	2.39E+06	0.206	1.28E+06	187
-55.88	41.78	8.37E+06	0.253		96
-55.94	41.84		0.002	8.36E+06	90

Table 4.4 –Continues

Water + dioxane liquid mixture at x2 = 0.163

T_{meas}	$\|T_s\|$	J_L	Intercept	J_R	# drops
-56.10	41.40	9.67E+04	-0.009		106
-56.11	41.41	1.09E+05	-0.038		130
-56.23	41.53	6.80E+05	0.158	3.29E+05	158
-56.24	41.54	7.68E+06	0.057	1.69E+07	130
-56.34	41.64	4.42E+05	0.126		155
-56.35	41.65	7.95E+06	0.118		86
-56.36	41.66	1.07E+07	0.284		261
-56.51	41.81	1.39E+05	-0.014		84
-56.70	42.00	3.57E+05	-0.045		110
-56.85	42.15	1.54E+07	0.092		60
-56.96	42.26	1.04E+06	0.125		238

Water + dioxane liquid mixture at x2 = 0.207

T_{meas}	$\|T_s\|$	J_L	Intercept	J_R	# drops
-55.16	45.884	2.12E+06	0.047		53
-55.31	46.034	4.05E+06	0.306		161
-55.51	46.234			5.76E+06	176
-55.80	46.524		0.544	9.72E+06	226
-55.88	46.604	1.85E+07	0.356		68
-56.08	46.804	6.45E+06	0.186		89
-56.22	46.944			2.27E+07	124
-56.29	47.014		0.325	1.33E+07	150
-56.31	47.034	1.40E+07	0.468		69
-56.63	47.354			5.14E+07	151
-56.88	47.604	1.06E+07	0.202	4.56E+07	200

Table 4.4 –Continues

Water + dioxane liquid mixture at x2 = 0.300

T_{meas}	$\|T_s\|$	J_L	Intercept	J_R	# drops
-51.14	49.02	1.27E+07	0.605	5.45E+05	140
-51.44	49.32	1.56E+06	-0.156	5.05E+05	130
-51.84	49.72		1.375	1.33E+07	189

Water + dioxane liquid mixture at x2 = 0.363

T_{meas}	$\|T_s\|$	J_L	Intercept	J_R	# drops
-51.61	51.81	1.90E+06	-0.036	8.18E+04	84
-51.68	51.88	4.64E+06	0.190		82
-51.70	51.90	6.03E+06	0.416		263
-51.72	51.92	2.70E+06	0.119	1.17E+06	139
-51.84	52.04	2.54E+06	0.132		114
-51.87	52.07	1.79E+06	0.114		131
-52.03	52.23	3.65E+06	0.127	1.10E+06	250
-52.04	52.24	2.63E+06	0.090		186
-52.11	52.31	1.41E+06			70
-52.12	52.32	3.03E+06	0.342	5.22E+05	108
-52.14	52.34		0.670	3.73E+06	114
-52.24	52.44	2.15E+06	0.040		117
-52.26	52.46	1.85E+06	0.076		185
-52.27	52.47		0.334	1.50E+07	158
-52.41	52.61	2.25E+06	0.171		190
-52.75	52.95	7.68E+05	-0.106		58

Water + dioxane liquid mixture at x2 = 0.477

T_{meas}	$\|T_s\|$	J_L	Intercept	J_R	# drops
-36.92	39.37	1.73E+06	0.140		145
-47.06	49.51	2.51E+06	0.379		125
-47.69	50.14		0.497	3.73E+07	43

A-) Measurements at $x_2 = 0.04$

At this mol fraction of dioxane, the measurements were performed in both traps at different times. The conversion $T_{comp.} = T_{meas.} - 0.8$ °C (Trap B) should be taken into account for the comparison of measurements in trap B to those in trap A.[3]

The ln (N_u/N_0) vs. $V_d \cdot t$ diagrams show patterns that are likely to represent surface nucleation, for the warmer end of the temperature intervals (trap A) at this composition. These kinds of statistics are described by the feature (**v**) within the context of this study.

If the "freezing time" vs. "index of droplet" diagrams in Appendix D are carefully examined, it is seen that the nucleation times tend to increase with decreasing temperature, for the temperatures T-meas: -43.19, -43.29, -43.31 -43.41°C. Strong dependence of nucleation times to the droplet volume is also observed for these types of statistics. In some experiments (T = -43.31, -43.43, -43.62, -43.36, -44.67, -44.99 °C), the nucleation time of droplets are altered with evolving experimental run-time, which can also be followed from the "freezing time" vs. "index of droplet" diagrams.

The increase of nucleation times with decreasing temperature, the strong dependence of nucleation times to droplet volumes and the shape of the ln (N_u/N_0) vs. $V_d \cdot t$ diagrams can be explained in two ways: In the first case the presence of an impurity, such as a tensile material, should be considered. The impurity can inhibit the formation of critical germ while it is diffusing out on the surface of droplet. When the impurities reach to the surface, they may lead to a surface structuring, hence triggering heterogeneous nucleation. In the second case a phase separation is considered between dioxane and water molecules. The occurrence of a phase separation prior to nucleation can also be figured out by time dependent (progressive) nucleation rates.

As the temperature decreases down, the feature (**v**) disappears; however "knick"s start to develop in the the ln(N_u/N_0) vs. $V_d \cdot t$ diagrams. Left to the knicks (short-time regions) have higher slopes resulting in higher nucleation rates in these diagrams. This finding does not eliminate the

[3] It should not be confused that only the **measurement** temperatures are given below the figures in the appendices.

presence of a time dependent nucleation rate discussed above; however implies a change in the nucleation mechanism. Finally, there are two other measurements which were performed at an unexpectedly high degree of supercooling (T = 47.54 & 47.64 °C – see Appendix D) at this mol fraction of dioxane; yet these results require to be reproduced to be signified.

B-) Measurements near the Eutectic Point

The nucleation rate measurements near the eutectic composition were conducted at $x_2 = 0.133$ and $x_2 = 0.163$. At these two concentrations the equilibrium melting points are equal. The $\ln(N_u/N_0)$ vs. $V_d \cdot t$ diagrams are usually broken at high $V \cdot t$ values (long-time regions) with the formation of knicks. This feature is more persistently observed at $x_2 = 0.133$ and usually at the warmer ends of the temperature intervals (cf. Appendix D). Right to the knicks have higher slopes, i.e. higher nucleation rates. This is in an opposite manner to that observed previously in the measurement of nucleation rates for pure H_2O.

C-) Measurements at Higher Dioxane Concentrations

The nucleation rate measurements at higher dioxane concentrations are performed at $x_2 = 0.207$, 0.300, 0.363 and 0.477. At these dioxane concentrations the stoichiometric ratio is more than 1 dioxane molecule per 5 water molecules. As a result the liquids water's network structure is disturbed to a great extent.

In examining the $\ln(N_u/N_0)$ vs. $V_d \cdot t$ diagrams (cf. Appendix D), it is seen that the nucleation statistics start to alter beyond $x_2 = 0.300$. In particular, very long-living droplets can be identified in the "freezing time" vs "index of droplet" diagrams. This leads to formation of knicks with right side having lower slopes, which is similar to observations made for pure water.

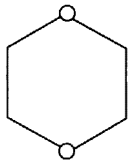

1,4-dioxane
M.W.:88.10
Boiling Point: 101.1 °C
Melting Point:11.85 °C

Ethanol
M.W.:46.07
Boiling Point: 78.35 °C
Melting Point:-114.35 °C

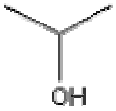

Isopropanol
M.W.:60.10
Boiling Point: 82.35 °C
Melting Point: -88.5 °C

Glycol
M.W.:62.07
Boiling Point: 197.35
Melting Point:-12.15 °C

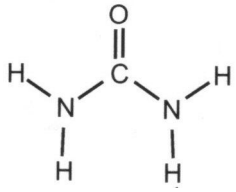

Urea
M.W.:60.06
Boiling Point:
Melting Point:132.8 °C

Figure 4.10: Molecular structures of non-electrolyte solutes; dioxane, ethanol, isopropanol, glycol and urea.